Supporting Information

Visualization of *NRAS* RNA G-Quadruplex Structures in Cells with an Engineered Fluorogenic Hybridization Probe

Shuo-Bin Chen,[†] Ming-Hao Hu,[†] Guo-Cai Liu,[†] Jin Wang,[‡] Tian-Miao Ou,[†] Lian-Quan Gu,[†] Zhi-Shu Huang,*[, †] and Jia-Heng Tan*[, †]

[†] School of Pharmaceutical Sciences, Sun Yat-sen University, Guangzhou 510006, China

[‡] Guangzhou Institute of Geochemistry, Chinese Academy of Sciences, Guangzhou 510640, China

Table of Contents:

1. Experimental Section

1.1 Synthesis and Characterization

Scheme S1. Synthesis of **ISCH-oa1** [a]

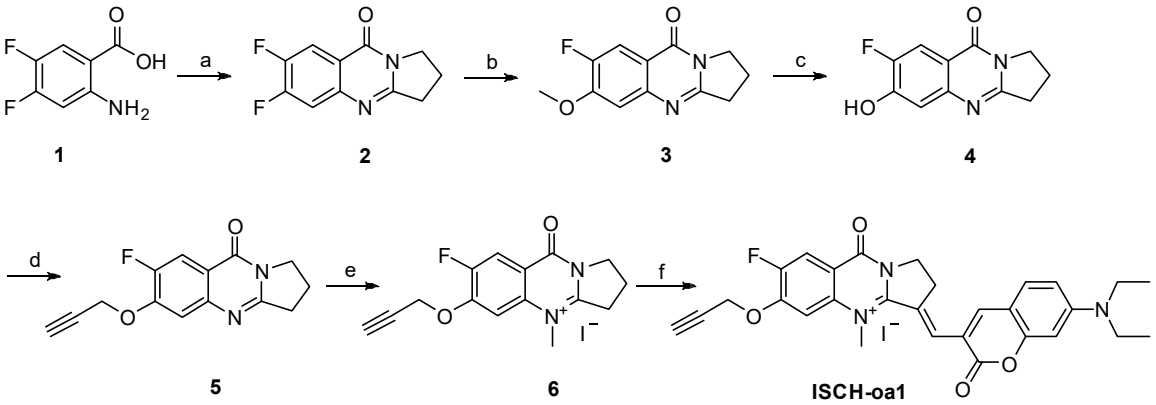

[a] **Reagents and conditions:** (a) pyrrolidin-2-one, $POCl_3$, 110 °C, 7 h; (b) CH_3ONa, CH_3OH, 60 °C, 24 h; (c) HBr, CH_3COOH, reflux, 24 h; (d) propargyl bromide, K_2CO_3, acetone, 50 °C, 15 h; (e) CH_3I, tetramethylene sulfone, 60 °C, 20 h; (f) 7-diethylaminocoumarin-3-aldehyde, EtOH, reflux, 12 h.

^{1}H and ^{13}C NMR spectra were recorded by using TMS as the internal standard in DMSO or $CDCl_3$ at 400 MHz and 100 MHz, respectively, with a Bruker BioSpin GmbH spectrometer. Mass spectra (MS) were recorded on a Shimadzu LCMS-2010A instrument with an ESI or ACPI mass selective detector and high resolution mass spectra (HRMS) were recorded on a Shimadzu LCMS-IT-TOF. Flash column chromatography was performed with silica gel (200–300 mesh) purchased from Qingdao Haiyang Chemical Co. Ltd. The purity of the synthesized compound was confirmed to be higher than 95% by using analytical HPLC performed with a dual pump Shimadzu LC-20 AB system equipped with a Ultimate XB-C18 column (4.6 × 250 mm, 5 μm) and eluted with methanol-water (80: 20) containing 0.1% TFA at a flow rate of 1.0 mL/min. All chemicals were purchased from commercial sources unless otherwise specified. All the solvents were of analytical reagent grade and were used without further purification.

Synthesis of 6,7-difluoro-2,3-dihydropyrrolo[2,1-*b*]quinazolin-9(1*H*)-one (2): To a mixture of 2-amino-4,5-difluorobezoic acid (3.34 g, 19.3 mmol) and pyrrolidin-2-one (3.00 mL, 39.5 mmol), 45 mL of $POCl_3$ was carefully added at room temperature. The mixture was then stirred at 110 °C for 7 h. After $POCl_3$ was removed under reduced pressure, the residue was poured into ice water, and then solution of NaOH was added to make the solution basic. The mixture was extracted with 3×50 mL portions of CH_2Cl_2. The combine organic phase

was dried over $MgSO_4$ and concentrated under reduced pressure. The crude product was purified by using flash column chromatography with EtOAc/petroleum ether (1 : 4) elution to afford a white solid (**2**, 2.81 g, yield 65%): ^{1}H NMR (400 MHz, $CDCl_3$) δ 8.02 (t, *J* = 9.2 Hz, 1H), 7.49-7.34 (m, 1H), 4.20 (t, *J* = 7.1 Hz, 2H), 3.17 (t, *J* = 7.8 Hz, 2H), 2.37-2.23 (m, 2H). ESI-MS m/z: 223.1 $[M+H]^+$.

Synthesis of 7-fluoro-6-methoxy-2,3-dihydropyrrolo[2,1-*b*]quinazolin-9(1*H*)-one (3): In the solution of compound **2** (1.00 g, 4.5 mmol) in CH_3OH (20 mL), CH_3ONa (1.00 g, 18.5 mmol) was suspended. Then the mixture was stirred at 60 °C for 24 h until the starting material disappeared. After that, the solid was removed through filtration, and the remaining solution was concentrated under reduced pressure. Then the crude product was washed by water and further dried to get a pale purple solid (**3**, 0.90 g, yield 85%): ^{1}H NMR (400 MHz, $CDCl_3$) δ 7.89 (d, *J* = 11.0 Hz, 1H), 7.13 (d, *J* = 7.5 Hz, 1H), 4.20 (t, *J* = 7.2 Hz, 2H), 3.98 (s, 3H), 3.17 (t, *J* = 7.9 Hz, 2H), 2.39 – 2.23 (m, 2H). ESI-MS m/z: 235.1 $[M+H]^+$.

Synthesis of 7-fluoro-6-hydroxy-2,3-dihydropyrrolo[2,1-*b*]quinazolin-9(1*H*)-one (4): Compound **3** (1.00 g, 4.3 mmol) was suspended into the solution of CH_3COOH (5 ml) and HBr (47%, 5 mL) and then the mixture was stirred at reflux for 24 h. After cooling, the mixture was treated with NaOH (aq) to reach the pH of 5, and the mixture was filtered to get a white solid (**4**, 0.64 g, yield 68%): ^{1}H NMR (400 MHz, DMSO-d_6) δ 7.70 (d, *J* = 11.1 Hz, 1H), 7.05 (d, *J* = 8.0 Hz, 1H), 4.022 (t, *J* = 7.4 Hz, 2H), 3.03 (t, *J* = 7.8 Hz, 2H), 2.25 – 2.07 (m, 2H). ESI-MS m/z: 221.1 $[M+H]^+$.

Synthesis of 7-fluoro-6-(prop-2-yn-1-yloxy)-2,3-dihydropyrrolo[2,1-*b*]quinazolin-9(1*H*)-one (5): Propargyl bromide (0.40 mL, 5.0 mmol) was added to a solution of **4** (1.00 g, 4.5 mmol) and anhydrous K_2CO_3 (0.69 g, 5.0 mmol) in 20 mL acetone. The resulting mixture was heated at 50 °C for 15 h until the reaction was complete, and then the solid was filtered away. After that, the remaining solution was concentrated under reduced pressure. Then 50 mL water was added, and the mixture was then extracted by ethyl acetate (3 × 50 mL). The organic layer was dried over Na_2SO_4 and concentrated to get a white solid (**5**, 0.82 g, yield 70%). ^{1}H NMR (400 MHz, $CDCl_3$) δ 7.85 (d, *J* = 10.8 Hz, 1H), 7.22 (d, *J* = 7.4 Hz, 1H), 4.80 (s, 2H), 4.13 (t, *J* = 7.2 Hz, 2H), 3.10 (t, *J* = 7.9 Hz, 2H), 2.52 (s, 1H), 2.29 – 2.15 (m, 2H). ESI-MS m/z: 259.1 $[M+H]^+$.

Synthesis of 7-fluoro-4-methyl-9-oxo-6-(prop-2-yn-1-yloxy)-1,2,3,9-tetrahydropyrrolo[2,1-*b*]quinazolin-4-ium (6): A solution of **5** (0.50 g, 1.9 mmol) in tetramethylene sulfone (2.0 mL) was treated with CH_3I (1.0

mL, 16.0 mmol). The mixture was heated at 60 °C for 20 h. After cooling, the mixture was filtered, and the crude product was washed with anhydrous ether and dried under vacuum to afford the product as a white solid (**6**, 0.52 g, yield 67%). ^{1}H NMR (400 MHz, DMSO-d_6) δ 8.15 (d, J = 10.1 Hz, 1H), 7.71 (d, J = 6.3 Hz, 1H), 5.29 (s, 2H), 4.30 (t, J = 6.7 Hz, 2H), 4.00 (s, 3H), 3.81 (s, 1H), 3.70 (t, J = 7.3 Hz, 2H), 2.40 – 2.27 (m, 2H). ESI-MS m/z: 273.1 $[M-I]^+$.

Synthesis of (*E*)-3-((7-(diethylamino)-2-oxo-2H-chromen-3-yl)methylene)-7-fluoro-4-methyl-9-oxo-6-(prop-2-yn-1-yloxy)-1,2,3,9-tetrahydropyrrolo[2,1-b]quinazolin-4-ium (ISCH-oa1): A mixture of **6** (0.50 g, 1.2 mmol), 7-*N*,*N*-diethylaminocoumarin-3-aldehyde (0.36 g, 1.5 mmol), and EtOH (20 mL) was stirred at reflux for 12 h. After cooling to room temperature, the solution was removed under reduced pressure. The crude product was purified by using flash column chromatography with CH_3OH/CH_2Cl_2 (1 : 50) elution to afford brownish black solid (**7**, 0.56 g, yield 71%): ^{1}H NMR (400 MHz, DMSO-d_6) δ 8.30 (s, 1H), 8.12 (d, J = 10.2 Hz, 1H), 7.84 (s, 1H), 7.65 – 7.75 (m, 2H), 6.86 (d, J = 9.1 Hz, 1H), 6.64 (s, 1H), 5.30 (s, 2H), 4.35 – 4.19 (m, 5H), 3.83 (s, 1H), 3.59 – 3.44 (m, 4H), 3.39 – 3.31 (m, 2H), 1.16 (t, J = 6.8 Hz, 6H). ^{13}C NMR (100 MHz, DMSO-d_6) δ 160.36, 159.39, 156.86, 156.26, 152.55, 151.64, 151.12, 145.14, 139.04, 138.82, 131.71, 126.83, 113.23, 112.98, 112.87, 110.30, 108.37, 105.19, 96.39, 80.22, 77.29, 58.03, 46.64, 44.46, 41.26, 27.67, 12.38. Purity: 97% by HPLC. HRMS (ESI): calcd for $[M-I]^+$ ($C_{29}H_{27}FN_3O_4^+$) 500.1980, found 500.1973.

Scheme S2. Synthesis of **GTFH** probes [a]

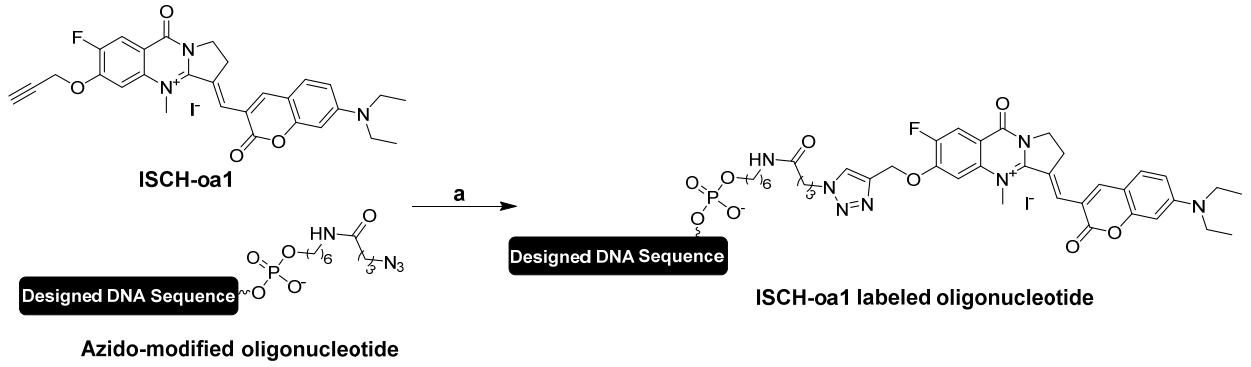

[a] **Reagents and conditions:** (a) water, sodium ascorbate, copper sulfate, 37°C, 24 h.

General Synthesis of GTFH probes: ISCH-oa1 (1 mM) and azido-modified DNA oligonucleotide (0.05 mM) were mixed in water (200 μL) containing fresh sodium ascorbate (1.2 mM), copper sulfate (0.6 mM) was stirred at reflux for 24 h at 37°C. The purity was determined by using RP-HPLC-UV and mass spectrometry.

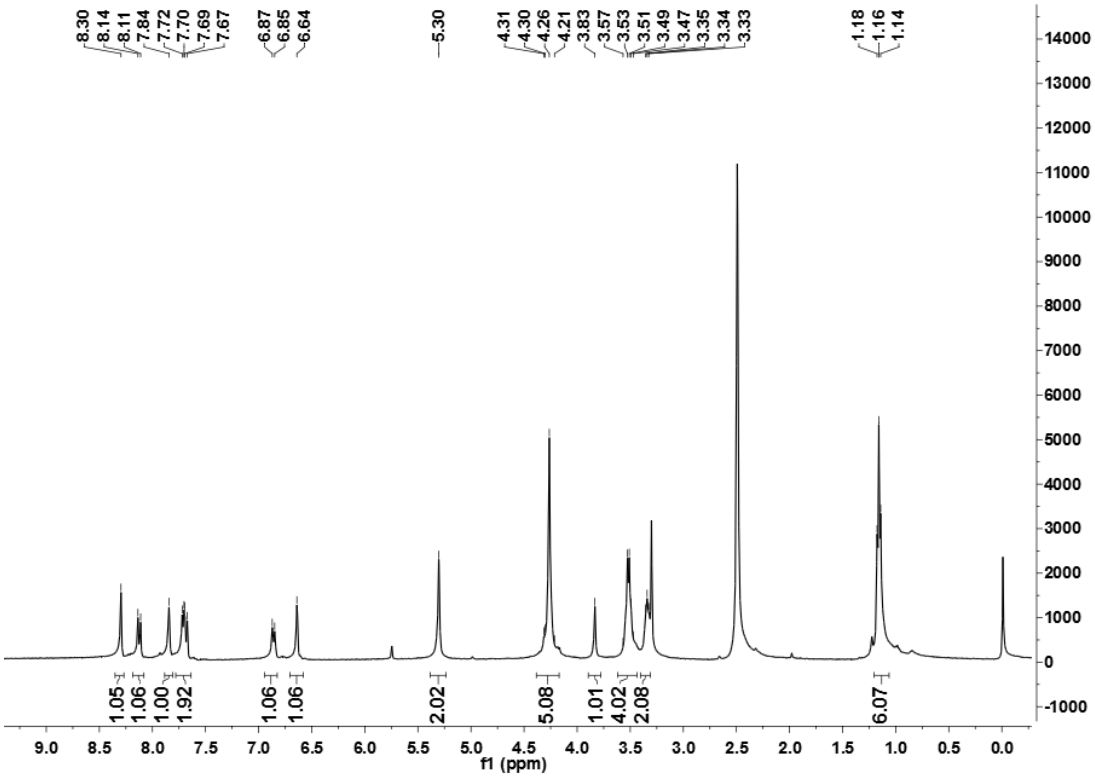

Figure S1. ^{1}H NMR spectrum of **ISCH-oa1**.

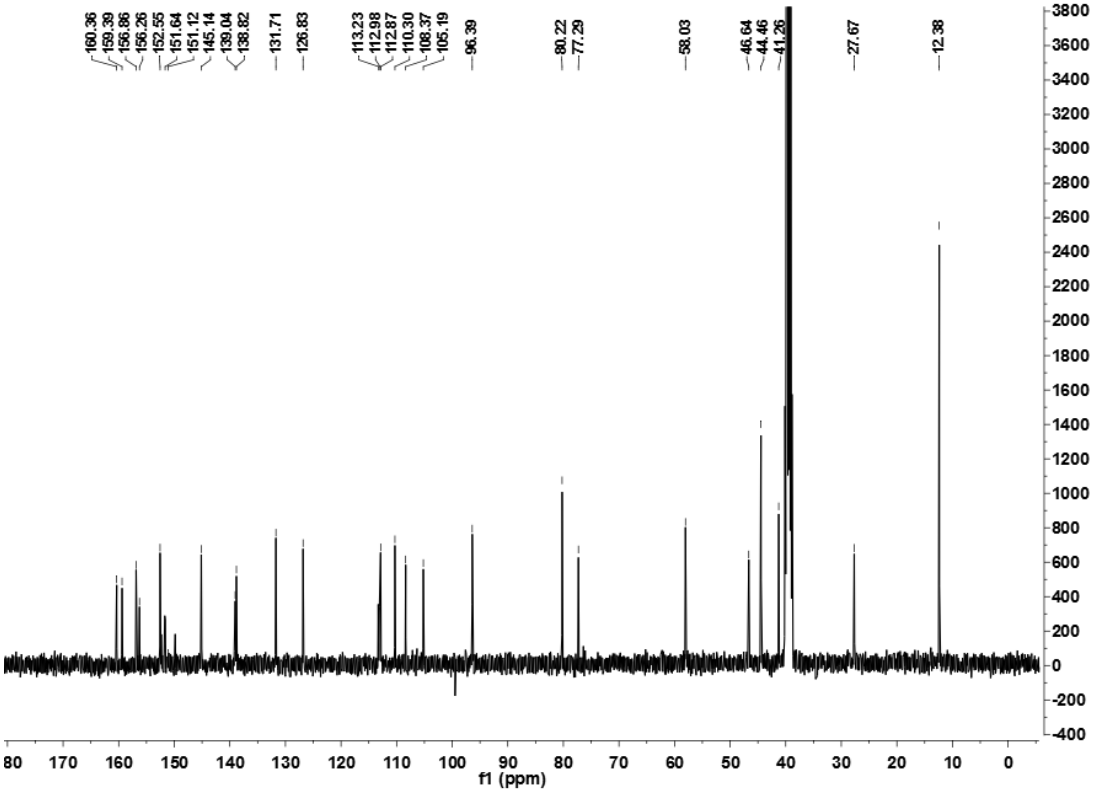

Figure S2.^{13}C NMR spectrum of **ISCH-oa1**.

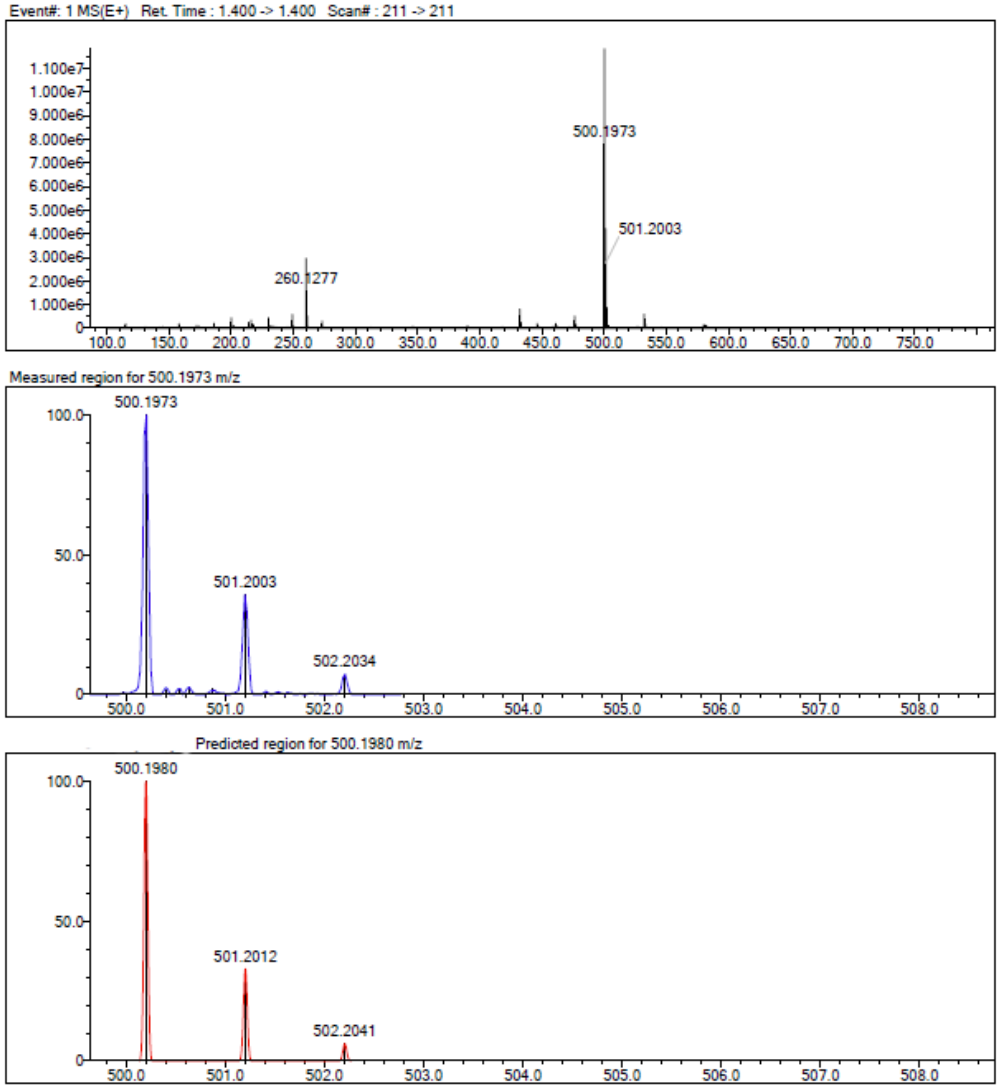

Figure S3. HRMS spectrum of **ISCH-oa1**.

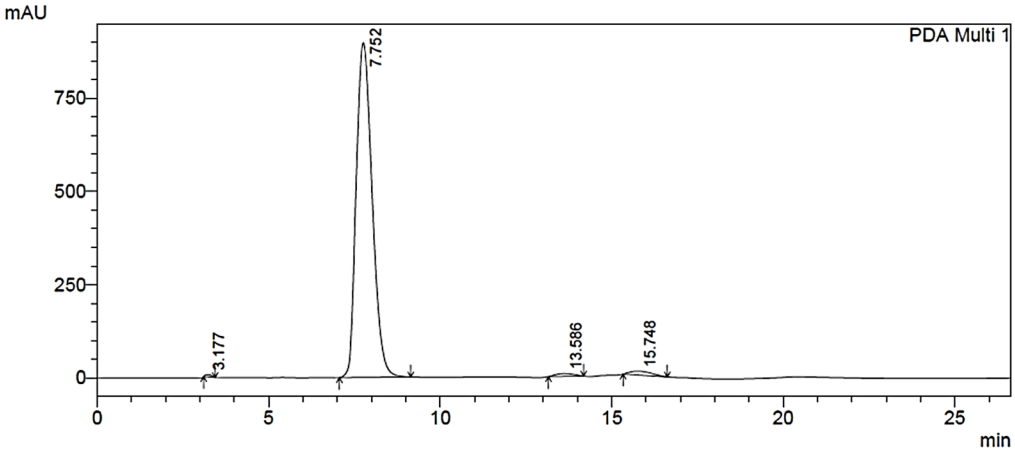

Figure S4. HPLC analysis of **ISCH-oa1**.

Table S1. Characterization of **GTFH** probes.

Name	Sequences	Target MS	Observed MS
ISCH-nras1	5′-d[ACCACGAGTCATGCGGCAGGCCGCA]-3′-**ISCH-oa1**	8454.6	8451.6
ISCH-r1	5′-d[ATCGACTACGCTTCACTACACCCTA]-3′-**ISCH-oa1**	8298.5	8295.6

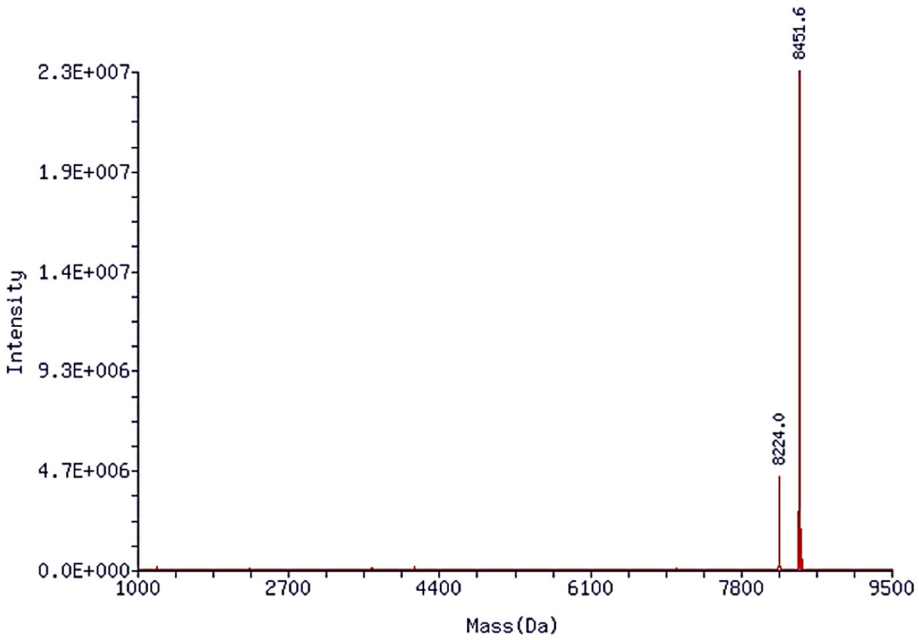

Figure S5. ESI mass spectrum of **ISCH-nras1**.

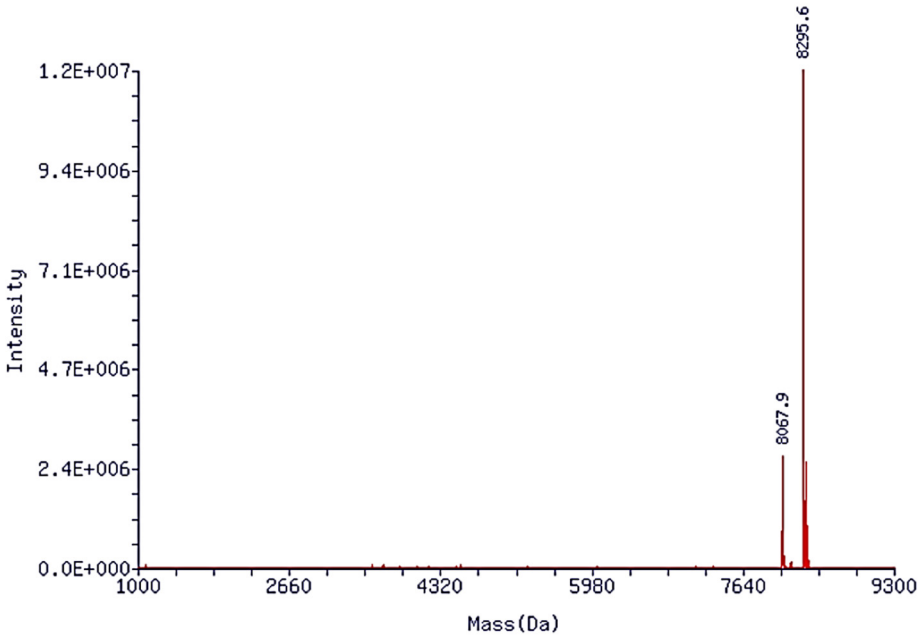

Figure S6. ESI mass spectrum of **ISCH-r1**.

1.2 CD Studies

Circular dichroism (CD) studies were performed on a Chirascan circular dichroism spectrophotometer (Applied Photophysics, UK). A quartz cuvette with a 1 cm path length was used for the recording of spectra over a wavelength range of 230–330 nm with a 1 nm bandwidth, 1 nm step size and time of 0.5 s per point. All oligonucleotides were annealed in relevant buffer by heating to 95 °C for 5 min, followed by gradual cooling to room temperature. CD melting was performed at a fixed concentration of different nucleic acid (1 μM), either with or without a fixed concentration (5 μM) of **IZCM-7** in Tris-HCl buffer (10 mM, pH 7.2) with 100 mM KCl. The data was recorded at intervals of 2.5 °C over a range of 25–95 °C, with a heating rate of 1.0 °C/min. A buffer baseline was collected in the same cuvette and was subtracted from the sample spectra. Final analysis of the data was conducted using Origin 7.0 (OriginLab Corp.).

1.3 TDS Studies

Thermal difference spectrum (TDS) studies were performed on a UV-2450 spectrophotometer (Shimadzu, Japan) using 1 cm path length quartz cuvette. All RNA oligonucleotides were diluted from stock to final concentration (1 μM) in Tris-HCl buffer (10 mM, pH 7.2) with 100 mM KCl. All samples were annealed by heating at 95°C for 5 min, gradually cooled to room temperature and measured after 24 h. UV-Vis spectra were recorded at 25 and 95 °C. A 10 min equilibration period at each measurement was allowed to ensure homogeneous sample temperature. TDS spectra were calculated by subtracting the spectrum at 25 °C from the spectrum at 95°C.

1.4 Electrophoretic Mobility Shift Assay (EMSA) Studies

Different oligonucleotides were loaded onto a 20% bisacrylamide gel in 1×TBE buffer containing 100 mM KCl and were electrophoresed at 4 °C. Oligonucleotides were stained by SYBR Gold and visualized under UV light and photographed using AlphaImager EC (Protein Simple).

1.5 Fluorescence Studies

Fluorescence studies were performed on QuantaMaster 400 Intensity Based Spectrofluorometer (PTI, USA). A quartz cuvette with 3 mm × 3 mm path length was used for the spectra recorded at 1 nm excitation and emission slit widths unless otherwise specified. Temperature-dependent fluorescence studies were performed on Chirascan circular dichroism spectrophotometer (Applied Photophysics, UK) equipped with a fluorometer accessory and a Peltier holder. The data was recorded at intervals of 5 °C over a range of 25–95 °C, with a heating rate of 1.0 °C/min.

1.6 Preparation of Long RNA Sequence

DNA fragments containing 5'-UTR sequence in *NRAS* mRNA and two restriction site, Nhe I/EcoR V were prepared by overlap PCR. The fragments were then inserted in the Nhe I site of the psiCHECK-2 vector (Promega, USA). Fragments containing 5'-UTR sequence were located between an upstream T7 promoter and a downstream EcoR V restriction site. Linear DNA with blunt end was prepared by cleavage of EcoR V site with Anza™ 26 Eco32I (Thermo Fisher Scientific, USA). The target RNAs were prepared by *in vitro* transcription following the Transcript Aid T7 High Yield Transcription Kit (Thermo Fisher Scientific, USA). The sequence of full-length *NRAS* 5′-UTR RNA fragments were list below.

UTR-full:

GCUAGCGAAACGUCCCGUGUGGGAGGGGCGGGUCUGGGUGCGGCCUGCCGCAUGACUCGUGG
UUCGGAGGCCCACGUGGCCGGGGCGGGGACUCAGGCGCCUGGGGCGCCGACUGAUUACGUAG
CGGGCGGGGCCGGAAGUGCCGCUCCUUGGUGGGGGCUGUUCAUGGCGGUUCCGGGGUCUCCA
ACAUUUUUCCCGGCUGUGGUCCUAAAUCUGUCCAAAGCAGAGGCAGUGGAGCUUGAGGUUCU
UGCUGGUGUGAAGAU

UTR-mutG:

GCUAGCGAAACGUCCCGUGUAAAAAAAGCGAGUCUGGGUGCGGCCUGCCGCAUGACUCGUGG
UUCGGAGGCCCACGUGGCCGGGGCGGGGACUCAGGCGCCUGGGGCGCCGACUGAUUACGUAG
CGGGCGGGGCCGGAAGUGCCGCUCCUUGGUGGGGGCUGUUCAUGGCGGUUCCGGGGUCUCCA
ACAUUUUUCCCGGCUGUGGUCCUAAAUCUGUCCAAAGCAGAGGCAGUGGAGCUUGAGGUUCU
UGCUGGUGUGAAGAU

UTR-delG:

GCUAGCGAAACGUCCCGUGCGGCCUGCCGCAUGACUCGUGGUUCGGAGGCCCACGUGGCCGG
GGCGGGGACUCAGGCGCCUGGGGCGCCGACUGAUUACGUAGCGGGCGGGGCCGGAAGUGCCG
CUCCUUGGUGGGGGCUGUUCAUGGCGGUUCCGGGGUCUCCAACAUUUUUCCCGGCUGUGGUC
CUAAAUCUGUCCAAAGCAGAGGCAGUGGAGCUUGAGGUUCUUGCUGGUGUGAAGAU

UTR-mT25:

GCUAGCGAAACGUCCCGUGUGGGAGGGGCGGGUCUGGGUACAACCUACCACAUAACUCAUAA
UUCGGAGGCCCACGUGGCCGGGGCGGGGACUCAGGCGCCUGGGGCGCCGACUGAUUACGUAG
CGGGCGGGGCCGGAAGUGCCGCUCCUUGGUGGGGGCUGUUCAUGGCGGUUCCGGGGUCUCCA

ACAUUUUUCCCGGCUGUGGUCCUAAAUCUGUCCAAAGCAGAGGCAGUGGAGCUUGAGGUUCU UGCUGGUGUGAAGAU

1.7 Cell Cultures and Hybridization Experiment in cells

The SiHa cells were grown in DMEM media containing 10% fetal bovine serum at 37 °C, with 5% CO_2 atmosphere. Cells were seeded in glass bottom 96-well plate (MatTek) and grew overnight. Oligonucleotide transfections were performed using 50 nM RNA oligonucleotides and Lipofectamine 3000 Transfection Reagent (Invitrogen, USA) for over 3 h. Cells were fixed with 4% paraformaldehyde in DEPC-PBS at room temperature for 15 min. After rinsing with DEPC-PBS, cells were permeabilized in 0.5% TritonX-100/DEPC/PBS at 37 °C for 30 min. After rinsing with 2X SSC, probes were diluted at 0.3 μM in hybridization buffer (4XSSC, 0.5 mM EDTA, 10% dextran sulfate, 30% deionized-formamide in DEPC-H2O) and applied to the cells. Hybridization was done at 37 °C overnight. After hybridization, cells were washed in 2XSSC for 15 min twice and subsequently stained with (0.5 $\mu g \cdot mL^{-1}$) DAPI for 15 min at 37 °C. For the RNase A treatment, cells were incubated with 200 $units \cdot mL^{-1}$ RNase A before hybridization at 37 °C for 1 h. For the RNase H treatment, cells were incubated with 200 $units \cdot mL^{-1}$ RNase H after hybridization at 37 °C for 1 h. Digital images were recorded using a LSM 710 laser scanning confocal microscope with a 63× objective lens, and analyzed with Imaris software (Bitplane Corp.).

1.8 Protein Extracts and Western Blotting

After 24 h treatment of **IZCM-7**, SiHa cells were harvested from each well. The cells were washed once with PBS and lysed with extraction buffer (50 mM glucose, 25 mM Tris-HCl, pH 8, 10 mM EDTA, 1 mM PMSF) at 4 ºC for 30 min. The lysed cells were centrifuged at 10,000 rpm at 4 °C for 5 min. The supernatant was transferred into another tube and the concentration of protein was calculated via BCA method. After boiled for 5 min at 95 °C with addition of loading buffer (50 mM Tris-HCl, pH 6.8, 6 M urea, 6% 2-mercaptoethanol, 3% SDS, 0.003% bromophenol blue), 20 μg of protein was loaded for each lane and resolved by SDS-PAGE and then transferred to a microporous polyvinylidene difluoride (PVDF) membrane and analyzed by Western blotting. Primary antibodies used for western blotting in this study were GAPDH (Beyotime Biotechnology: AF0006), NRAS (Aviva Systems Biology: OAEB02340). Secondary antibodies used were horseradish peroxidase-conjugated anti-mouse (Cell Signaling Technology: 7076S) or anti-rabbit (Cell Signaling Technology: 7074S). Protein bands were visualized using chemiluminescence substrate.

1.9 High-Content Imaging Studies

The SiHa cells were grown in DMEM media containing 10% fetal bovine serum at 37 °C, with 5% CO_2 atmosphere. Cells were seeded in glass bottom 96-well plate (MatTek) and grew overnight. pRNAT-U6.1/Neo vector (GenScript, USA) with DNA fragment containing 5'-UTR sequence in *NRAS* mRNA were transfected by Lipofectamine 3000 Transfection Reagent (Invitrogen, USA) for 24 h. Cells were fixed with 4% paraformaldehyde in DEPC-PBS at room temperature for 15 min. After rinsing with DEPC-PBS, cells were permeabilized in 0.5% TritonX-100/DEPC/PBS at 37 °C for 30 min. After rinsing with 2X SSC, probes were diluted at 1 μM in hybridization buffer (4XSSC, 0.5 mM EDTA, 10% dextran sulfate, 30% deionized-formamide in DEPC-H2O) and applied to the cells. Hybridization was done at 37 °C overnight. After hybridization, cells were washed in 2XSSC for 15 min twice and subsequently stained with (0.5 $\mu g \cdot mL^{-1}$) DAPI for 15 min at 37 °C. The Cellomics ArrayScan Vti (Thermo Fisher Scientific, USA) high-content imaging platform was used for the quantification of the fluorescence signal in cells. The high-content analysis automatically focused in the fluorescence channel of DAPI and captured the channel of **ISCH-nras1** with exposed time for 2s in the cytoplasm. Each sample contained about 10000 cells and three parallel experiments were performed.

2. Materials

Table S2. RNA and DNA samples used in the present study.

Name	Oligonucleotide Sequence
G4T25	5′-r[UGUGGGAGGGGCGGGUCUGGGUGCGGCCUGCCGCAUGACUCGUGGU]-3′
G4T25-mg1	5′-r[UGUAAGAGAAGCGAGUCUGAGUGCGGCCUGCCGCAUGACUCGUGGU]-3′
G4T25-mg2	5′-r[UGUAAAAAAAGCGAGUCUGAGUGCGGCCUGCCGCAUGACUCGUGGU]-3′
G4T25-mt1	5′-r[UGUGGGAGGGGCGGGUCUGGGUACAACCUACCACAUAACUCAUAAU]-3′
GT25	5′-r[GUGCGGCCUGCCGCAUGACUCGUGGU]-3′
G4d	5′-r[UGUGGGAGGGGCGGGUCUGGG]-3′
TERRA	5′-r[GGGUUAGGGUUAGGGUUAGGG]-3′
FAM-G4T25	5′-FAM-r[UGUGGGAGGGGCGGGUCUGGGUGCGGCCUGCCGCAUGACUCGUGGU]-3′
G4c	5′-d[CCCAGACCCGCCCCTCCCACA]-3′
P25c	5′-d[ACCACGAGTCATGCGGCAGGCCGCA]-3′
PU22	5′-d[TGAGGGTGGGTAGGGTGGGTAA]-3′
HTG22	5′-d[AGGGTTAGGGTTAGGGTTAGGG]-3′
HRAS	5′-d[TCGGGTTGCGGGCGCAGGGCACGGGCG]-3′
A647-nras1	5′-d[ACCACGAGTCATGCGGCAGGCCGCA]-3′-AlexaFluor647
Azido-nras1	5′-d[ACCACGAGTCATGCGGCAGGCCGCA]-3′-Azido
Azido-r1	5′-d[ATCGACTACGCTTCACTACACCCTA]-3′-Azido
dsG4T25	5′-d[TGTGGGAGGGGCGGGTCTGGGTGCGGCCTGCCGCATGACTCGTGGT]-3′ 3′-d[ACACCCTCCCCGCCCAGACCCACGCCGGACGGCGTACTGAGCACCA]-5′

All oligonucleotides used in this study were purchased from Invitrogen (China), TaKaRa (China) and Integrated DNA Technologies (USA). SYBR Gold was purchased from Thermo Fisher Scientific (USA). All the oligonucleotides were dissolved in relevant buffer. Their concentrations were determined from the absorbance at 260 nm, respectively on the basis of respective molar extinction coefficients using NanoDrop 1000 Spectrophotometer (Thermo Fisher Scientific, USA). To obtain G-quadruplex formation, oligonucleotides were annealed in relevant buffer containing KCl by heating to 95 °C for 5 min, followed by gradual cooling to room temperature. **IZCM-7** was prepared according to published procedures.[1] Stock solutions of compounds (10 mM) were dissolved in DMSO and stored at -80 °C. Further dilutions of samples to working concentrations were made with relevant buffer immediately prior to use.

3. Other Supporting Table, Spectra and Graphs

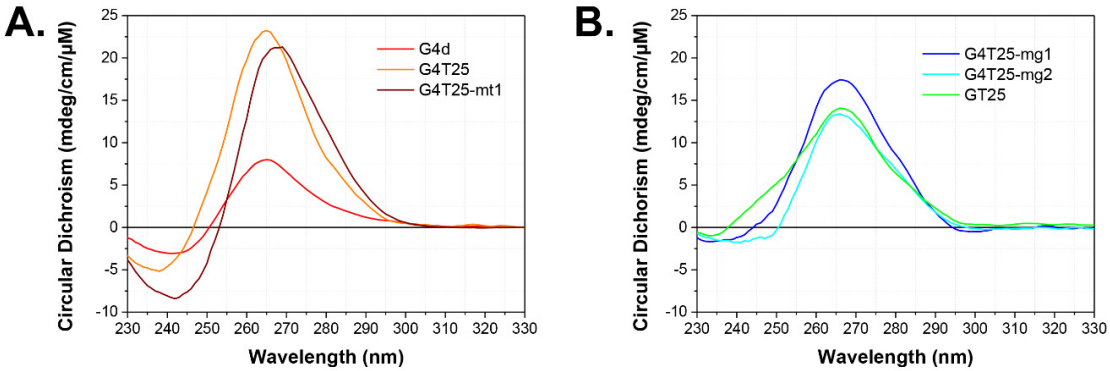

Figure S7. CD spectra of 1 μM RNAs in 10 mM Tris-HCl buffer, 100 mM KCl, pH 7.2. (A) RNAs with G-rich sequences. (B) RNAs with mutation or deletion of G-rich sequences. The CD profiles of the RNAs with G-rich sequences (**G4T25**, **G4T25-mt1** and **G4d**) showed a positive peak at around 265 nm, and a significant negative peak at around 240 nm. These peaks were typical signatures of G-quadruplex structures.[2]

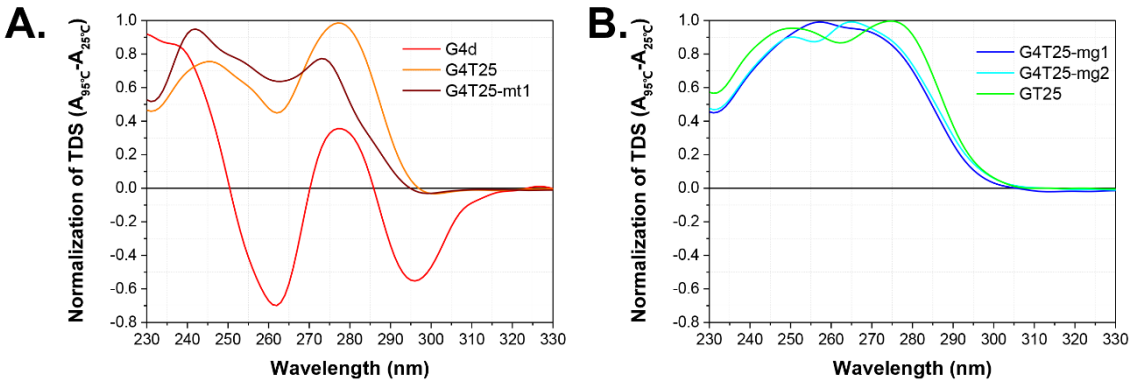

Figure S8. TDS studies of 1 μM RNAs in 10 mM Tris-HCl buffer, 100 mM KCl, pH 7.2. (A) RNAs with G-rich sequences. (B) RNAs with mutation or deletion of G-rich sequences. TDS studies were obtained by recording the UV absorbance spectra of the unfolded and folded states at temperatures above and below the melting temperature. The TDS profiles of the RNAs with G-rich sequences (**G4T25**, **G4T25-mt1** and **G4d**) showed two positive peaks at 240 nm and 275 nm, and a negative peak at 297 nm. These peaks were typical signatures of G-quadruplex structures.[3] By contrast, TDS profiles of sequences **G4T25-mg1**, **G4T25-mg2** and **GT25** were quite different. They could not form G-quadruplex structures.

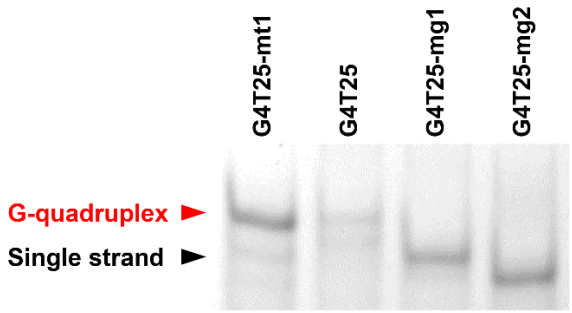

Figure S9. Electrophoresis staining of RNAs by SYBR Gold.

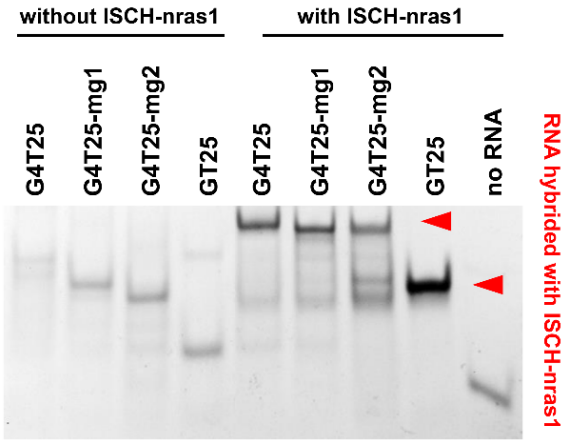

Figure S10. Electrophoresis staining of RNAs with or without **ISCH-nras1** by SYBR Gold.

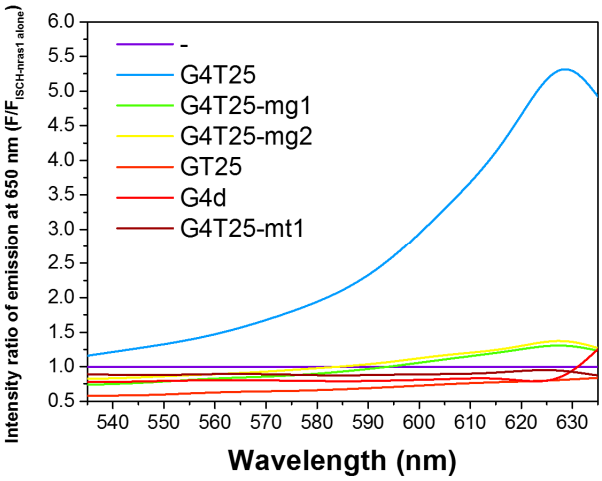

Figure S11. Relative fluorescence excitation spectra of 1 μM **ISCH-nras1** in 10 mM Tris-HCl buffer, 100 mM KCl, pH 7.2, with and without RNAs. Intensity ratio of emission at 650 nm ($F_{ISCH\text{-}nras1\ with\ RNAs}/F_{ISCH\text{-}nras1\ alone}$) were employed to determine the optimal excitation wavelength for distinguishing **G4T25** from other RNAs to the greatest extent possible. Obviously, 630 nm was the best excitation wavelength. Besides, 630 nm was also suitable for the laser scanning confocal microscope. Thus, 630 nm was chosen as the excitation wavelength for the fluorescence and cell imaging studies.

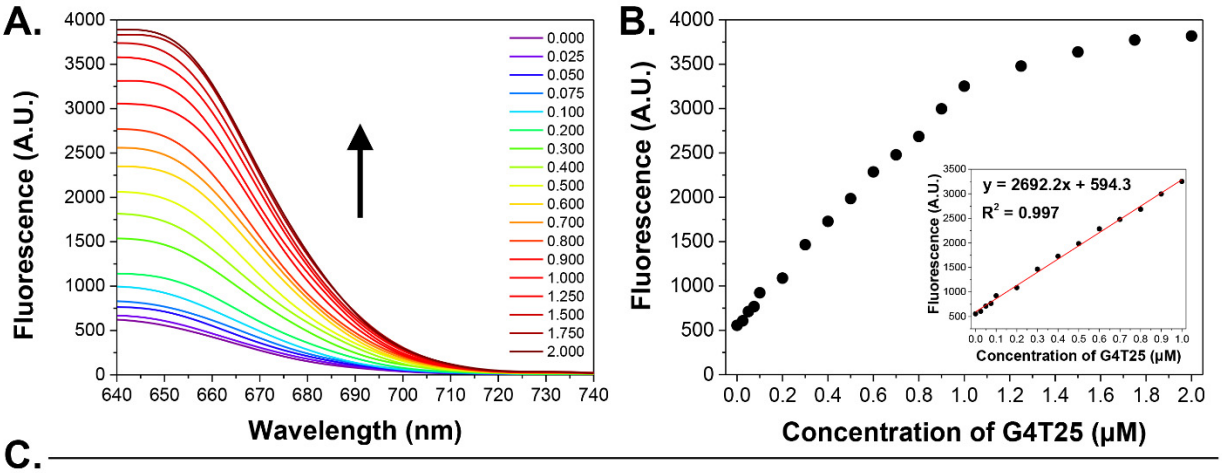

C.

Fluorescence Intensity of ISCH-nras1 with Different Amounts of G4T25

c (μM)	0.000	0.025	0.050	0.075	0.100	0.200	0.300	0.400	0.500	0.600	0.700	0.800	0.900	1.000	1.250	1.500	1.750	2.000
F	556	607	712	767	923	1088	1465	1728	1985	2286	2478	2685	2997	3253	3479	3638	3773	3818

Figure S12. Concentration-Dependent fluorescence emission of 1 μM **ISCH-nras1** with different amounts of **G4T25** in 10 mM Tris-HCl buffer, 100 mM KCl, pH 7.2, excited at 630 nm. (A) Fluorescence spectra of 1 μM **ISCH-nras1** with different amounts of **G4T25**. (B) The fluorescence emission change of 1 μM **ISCH-nras1** at 650 nm against different amounts of **G4T25**. Linear fit equation for calculating detection limit of **ISCH-nras1** for **G4T25** was plotted in the inner panel. The detection limit was then calculated on the basis of the equation "detection limit = $K \times S_b/m$".[1] The K value is generally taken to be 3 according to the IUPAC recommendation. The S_b value represents the standard deviation for multiple measurements (n = 20) of blank solution. The m value is the slope of the calibration curve, which is derived from the linear range of **ISCH-nras1** fluorescence titration curve with **G4T25** and represents the sensitivity of this method. The detection limit of **ISCH-nras1** for the RNA G-quadruplex formed by the **G4T25** was 0.024 μM. (C) Fluorescence emission data of 1 μM **ISCH-nras1** with different amounts of **G4T25** at 650 nm.

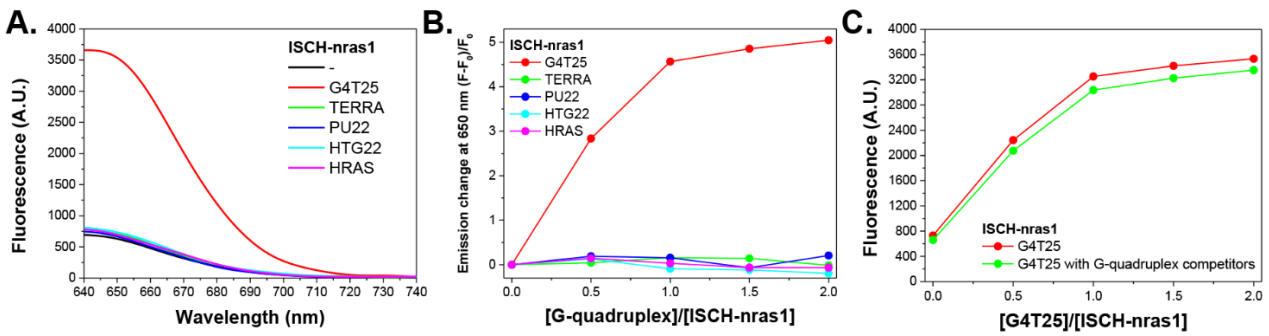

Figure S13. Fluorescence studies of the interactions of **ISCH-nras1** with different G-quadruplex structures in 10 mM Tris-HCl buffer, 100 mM KCl, pH 7.2, excited at 630 nm. (A) Fluorescence spectrum of 1 μM **ISCH-nras1** with or without 2 μM G-quadruplexs. (B) The fluorescence emission change of 1 μM **ISCH-nras1** at 650 nm against the ratio of [G-quadruplex]/[**ISCH-nras1**]. (C) The fluorescence titration of 1 μM **ISCH-nras1** with the stepwise addition of the **G4T25** without and with a mixture of G-quadruplex competitors containing 2 μM **TERRA**, **PU22**, **HTG22** and **HRAS**, respectively. While adding **G4T25** into the solution containing **ISCH-nras1** and other G-quadruplex structures, the enhanced fluorescence emissions were practically identical to those in the experiment without competitors. These results further confirmed attaching an oligonucleotide to the G-quadruplex probe that could hybridize with a sequence adjacent to the G-rich sequence of interest would improve its selectivity.

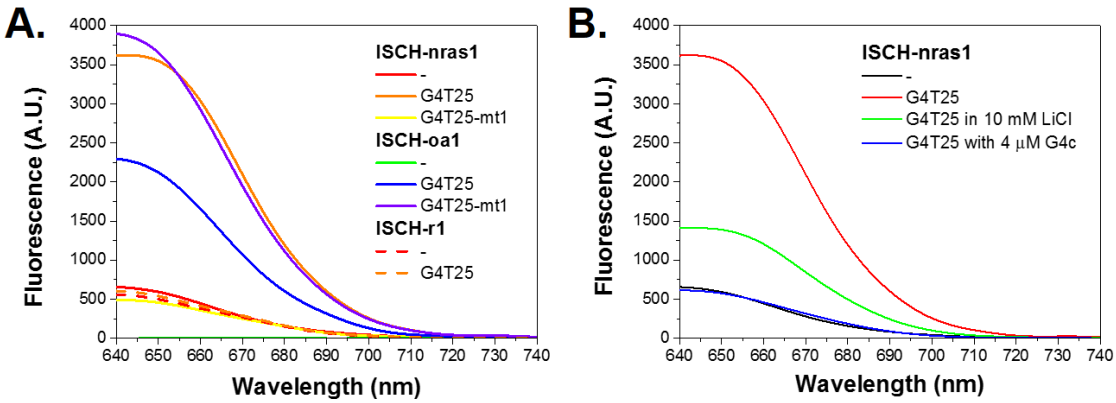

Figure S14. Fluorescence spectrum of 1 μM probes with and without RNAs excited at 630 nm. (A) Fluorescence spectra of different probes with or without **G4T25**, **G4T25-mt1** in 10 mM Tris-HCl buffer, 100 mM KCl, pH 7.2. (B) Fluorescence spectra of **ISCH-nras1** with or without **G4T25** in the present of LiCl or **G4c**. In the presence of lithium ions or the anti-sense C-rich DNA strand **G4c**, which is complementary strand to the G-rich sequence of **G4T25**, G-quadruplex structure in **G4T25** unwound.

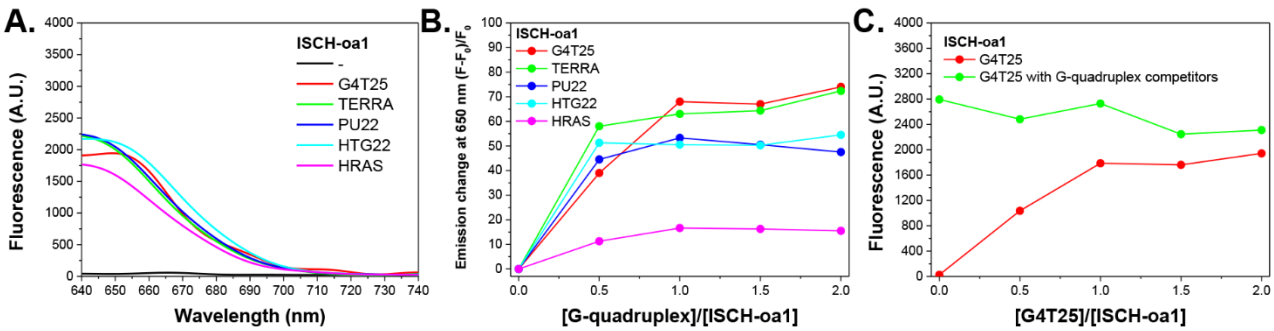

Figure S15. Fluorescence studies of the interactions of **ISCH-oa1** with different G-quadruplex structures in 10 mM Tris-HCl buffer, 100 mM KCl, pH 7.2, excited at 630 nm. (A) Fluorescence spectrum of 1 μM **ISCH-oa1** with or without 2 μM G-quadruplexs. (B) The fluorescence emission change of 1 μM **ISCH-oa1** at 650 nm against the ratio of [G-quadruplex]/[**ISCH-oa1**]. (C) The fluorescence titration of 1 μM **ISCH-oa1** with the stepwise addition of the **G4T25** without and with a mixture of G-quadruplex competitors containing 2 μM **TERRA**, **PU22**, **HTG22** and **HRAS**, respectively. The enhanced fluorescence emissions of **ISCH-oa1** were greatly affected by the G-quadruplex competitors.

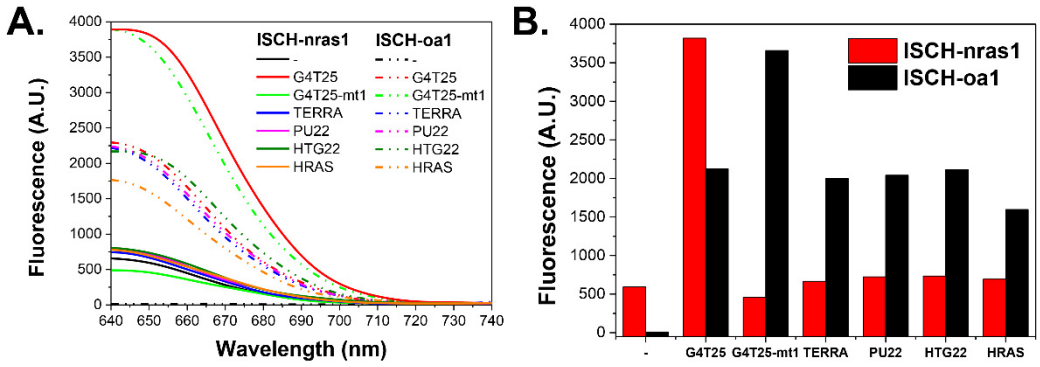

C.

	Fluorescence Intensity (A.U.)						
	-	G4T25	G4T25-mt1	TERRA	PU22	HTG22	HRAS
ISCH-nras1	594	3818	458	667	725	735	694
ISCH-oa1	10	2124	3658	1998	2042	2117	1597

Figure S16. Comparisons of the fluorescence emission of 1 μM **ISCH-nras1** and **ISCH-oa1** without (-) or with 2 μM different G-quadruplex structures in 10 mM Tris-HCl buffer, 100 mM KCl, pH 7.2, excited at 630 nm. (A) Fluorescence spectra of 1 μM **ISCH-nras1** and **ISCH-oa1** without (-) or with 2 μM different G-quadruplex structures. (B) Fluorescence emission of 1 μM **ISCH-nras1** and **ISCH-oa1** without (-) or with 2 μM different G-quadruplex structures at 650 nm. (C) Fluorescence emission data of 1 μM **ISCH-nras1** and **ISCH-oa1** without (-) or with 2 μM different G-quadruplex structures at 650 nm.

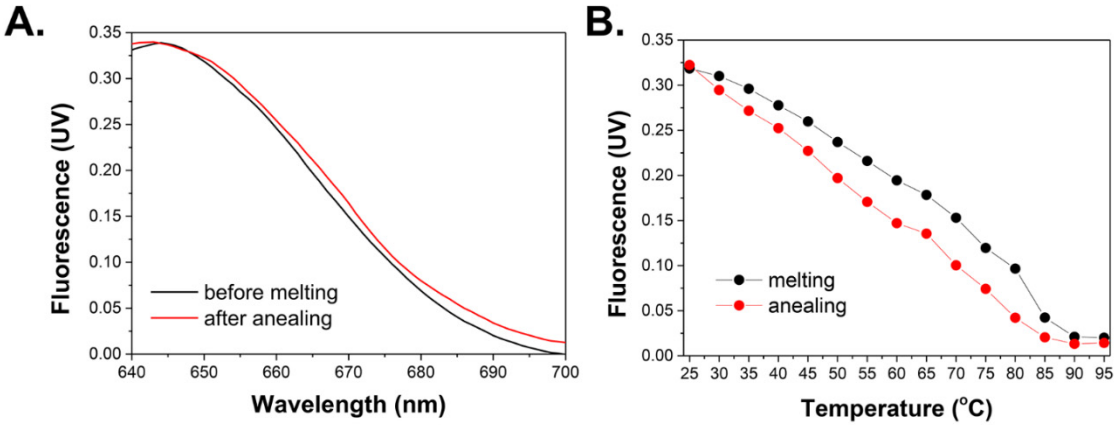

Figure S17. Temperature-Dependent fluorescence studies of **ISCH-nras1** with **G4T25** in 10 mM Tris-HCl buffer, 100 mM KCl, pH 7.2, excited at 630 nm. (A) Fluorescence spectrum of 5 μM **ISCH-nras1** with 5 μM **G4T25** before melting and after annealing process. (B) Fluorescence intensity of 5 μM **ISCH-nras1** with 5 μM **G4T25** during the melting or annealing process.

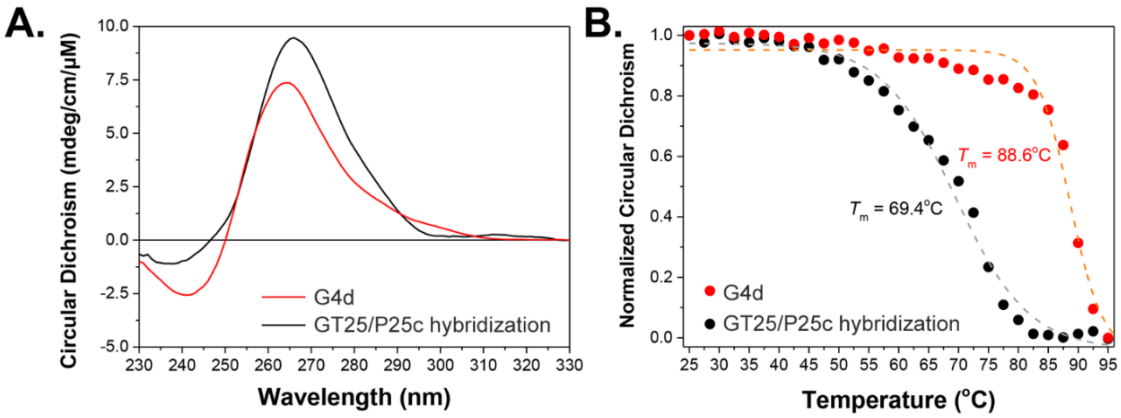

Figure S18. CD melting studies of 1 μM RNA G-quadruplex (**G4d**) and 1 μM DNA-RNA hybridization duplex (hybridization of **GT25** and **P25c**) in 10 mM Tris-HCl buffer, 100 mM KCl, pH 7.2. (A) CD spectra of the G-quadruplex and duplex structures. (B) Normalized CD signal of the G-quadruplex and duplex structures during melting process. The G-quadruplex in **G4d** was characterized by the positive peak at 265 nm, and the duplex in **GT25**/**P25c** was characterized by the positive peak at 270 nm. The melting point was calculated by the Boltzmann Formula.

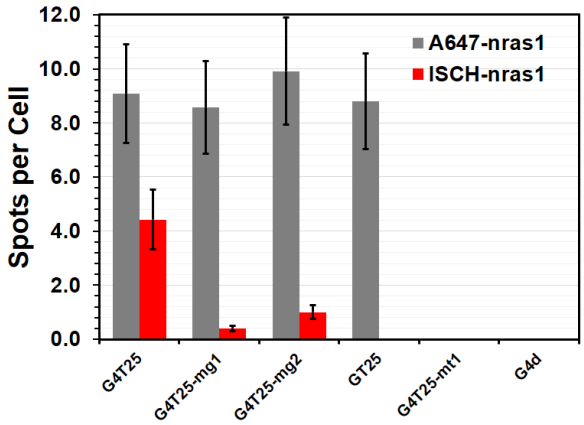

Figure S19. Quantification of **A647-nras1** and **ISCH-nras1** spots inside cells transfected with RNAs.

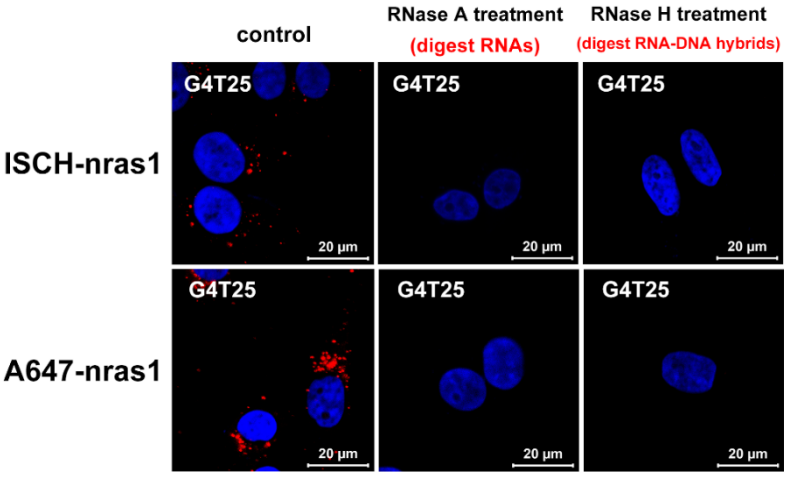

Figure S20. Confocal imaging of **G4T25**-transfected cells stained with **ISCH-nras1** and **A647-nras1** after RNase A and H treatment.

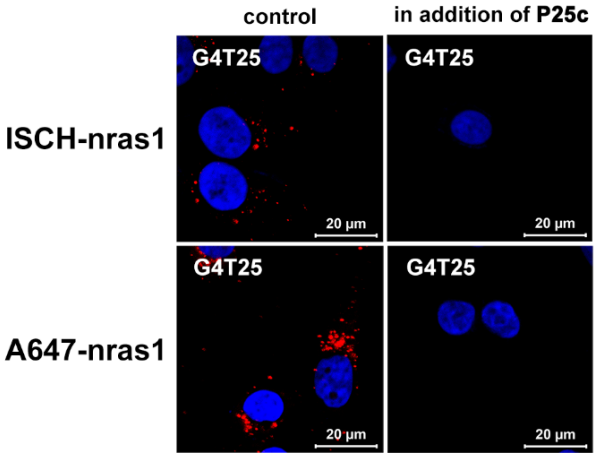

Figure S21. Confocal imaging of **G4T25**-transfected cells stained with **ISCH-nras1** and **A647-nras1** upon the addition of a complementary strand **P25c** to the tail sequence of **G4T25** in the staining processes.

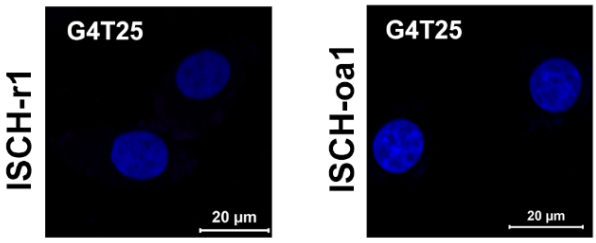

Figure S22. Confocal imaging of **G4T25**-transfected cells stained with **ISCH-r1** and **ISCH-oa1**.

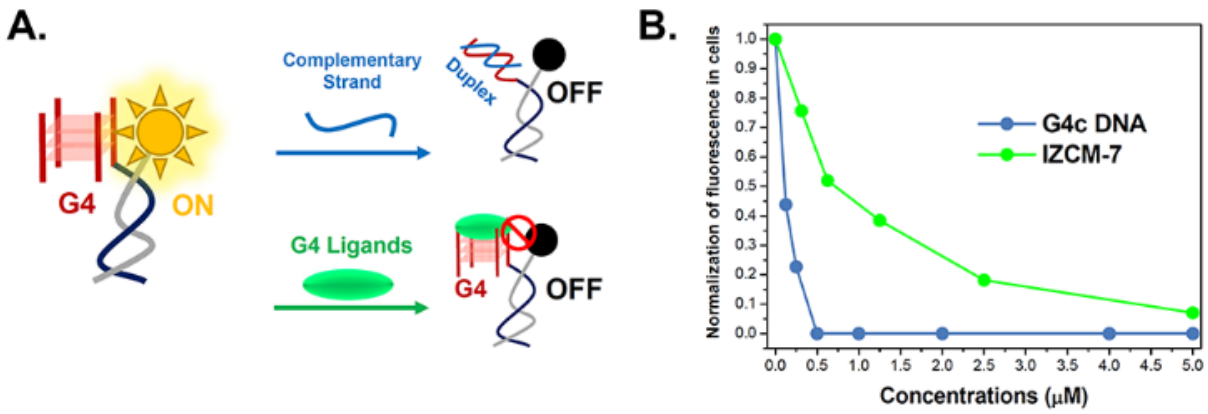

Figure S23. Effect of the complementary strand **G4c** and the G-quadruplex ligand **IZCM-7** on the visualization of the **G4T25** G-quadruplex structure by **ISCH-nras1**. (A) Illustration of the interactions. (B) Change in fluorescence inside the cells upon addition of **G4c** and **IZCM-7**.

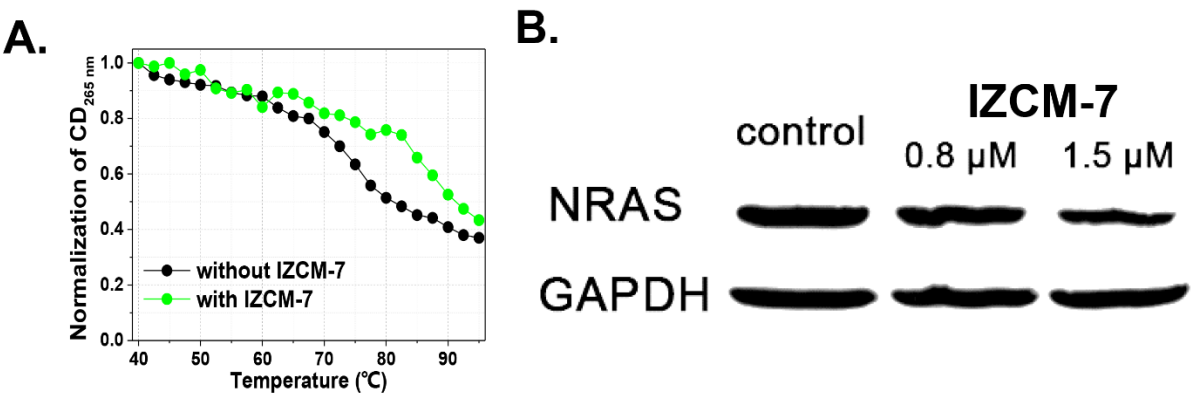

Figure S24. Evidence of **IZCM-7** binding to *NRAS* 5′-UTR G-quadruplex in cells. (A) CD melting curves of RNA **G4T25** with or without **IZCM-7**. (B) Expression of *NRAS* protein in SiHa cells with or without **IZCM-7**.

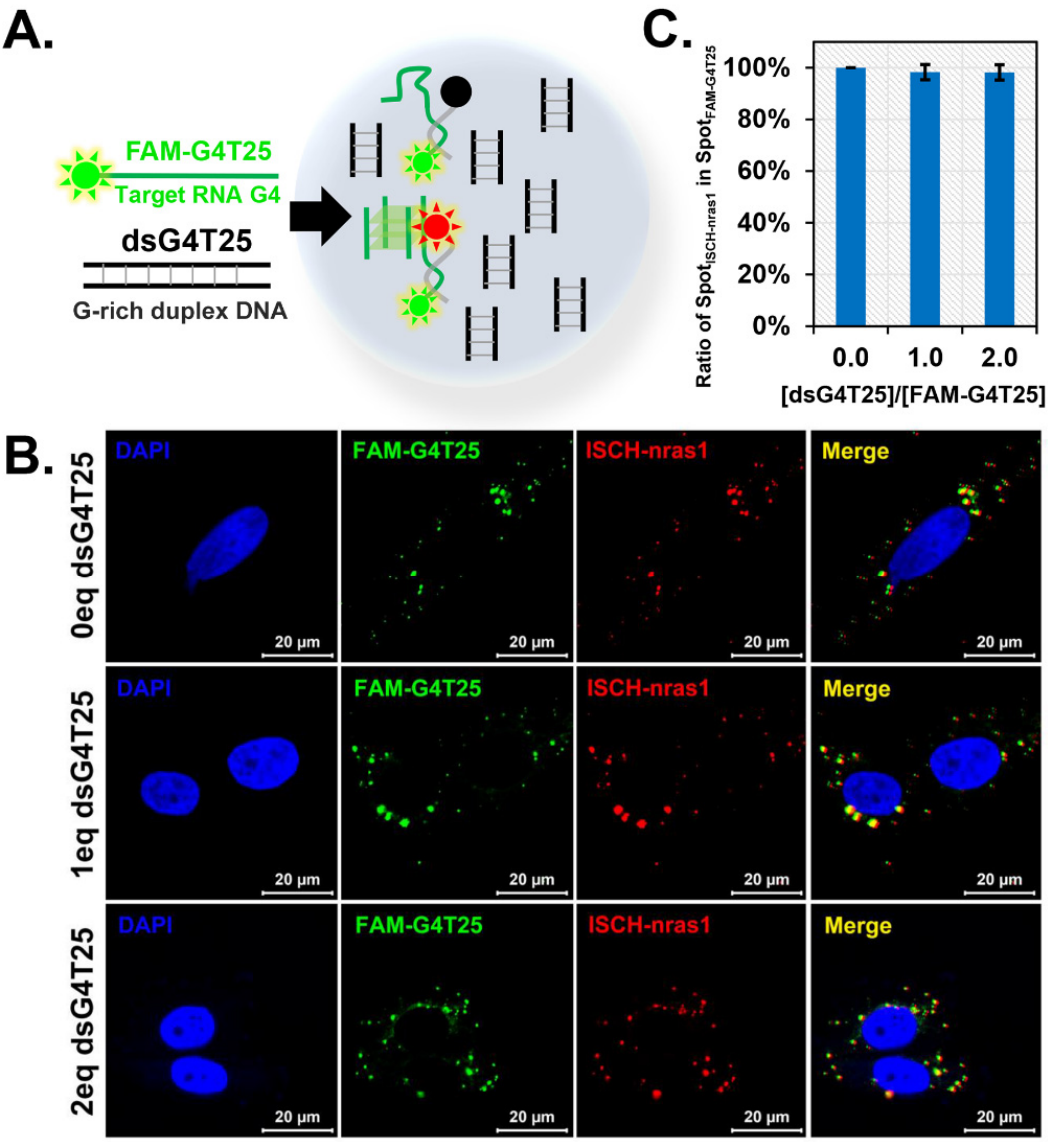

Figure S25. Effect of **dsG4T25** on the visualization of the **G4T25** G-quadruplex structure by **ISCH-nras1**. **dsG4T25** was a G-rich duplex competitor, whose sequence was identical to **G4T25**. (A) Illustration of the co-transfection and tracking of the RNAs in cells. (B) Confocal imaging of the effect of **dsG4T25** on the visualization of the **G4T25** G-quadruplex structure by **ISCH-nras1**. (C) Quantification of **ISCH-nras1** spots inside **FAM-G4T25** spots in cells.[4]

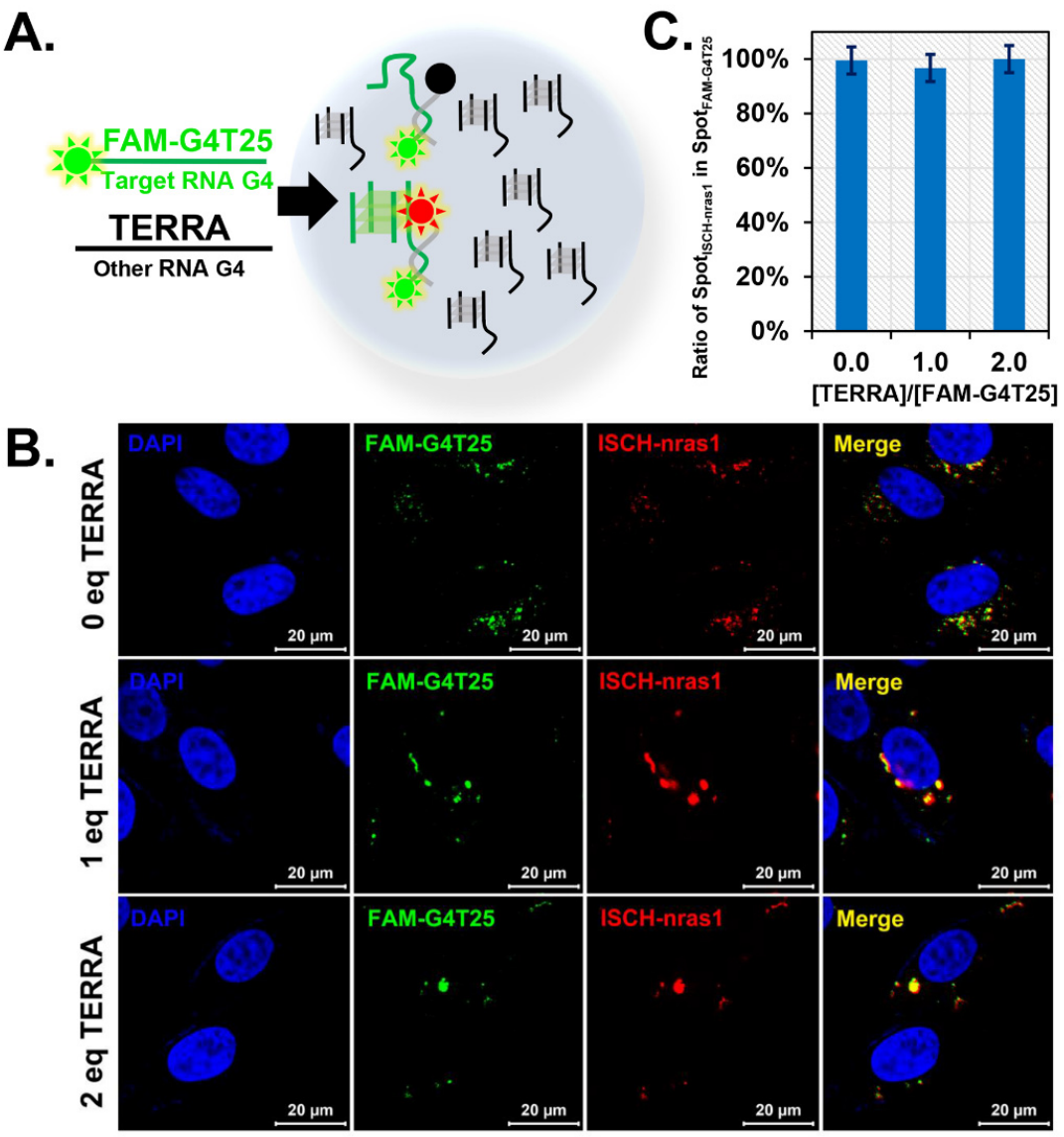

Figure S26. Effect of **TERRA** on the visualization of the **G4T25** G-quadruplex structure by **ISCH-nras1**. **TERRA** was a RNA G-quadruplex competitor. (A) Illustration of the co-transfection and tracking of the RNAs in cells. (B) Confocal imaging of the effect of **TERRA** on the visualization of the **G4T25** G-quadruplex structure by **ISCH-nras1**. (C) Quantification of **ISCH-nras1** spots inside **FAM-G4T25** spots in cells.

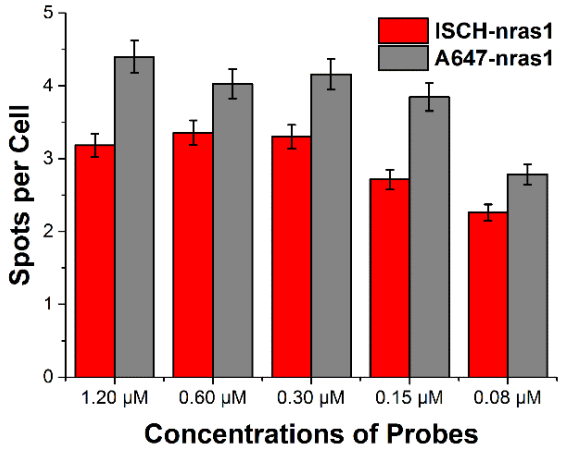

Figure S27. Quantification of spots inside cells transfected with **G4T25** stained by various concentrations of **A647-nras1** and **ISCH-nras1**. The fluorescence spots in cells were almost the same when concentration of **ISCH-nras1** or **A647-nras1** was above 0.3 μM. Thus, 0.3 μM of **ISCH-nras1** or **A647-nras1** was used in the cell staining assays.

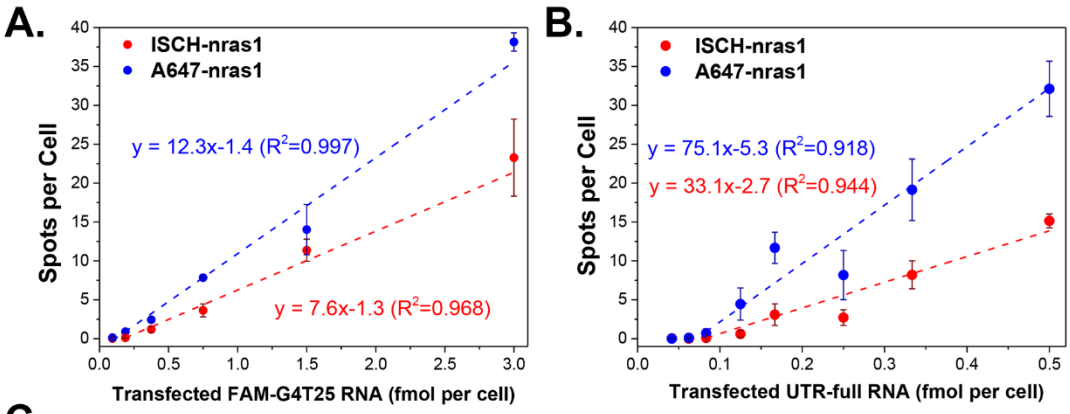

C.

Probe	linear range (fmol/cell)		detection limit (fmol/cell)	
	FAM-G4T25	UTR-full	FAM-G4T25	UTR-full
ISCH-nras1	0.1 - 3.0	0.08 - 0.5	0.30	0.11
A647-nras1	0.1 - 3.0	0.08 - 0.5	0.20	0.08

Figure S28. Quantification of **ISCH-nras1** and **A647-nras1** spots inside cells transfected with different amount of RNAs. (A) **ISCH-nras1** and **A647-nras1** spots per cell transfected with **FAM-G4T25**. (B) **ISCH-nras1** and **A647-nras1** spots per cell transfected with **UTR-full**. (C) The detection limits and linear ranges of **ISCH-nras1** and **A647-nras1** for the RNAs. The detection limit per cell was defined as the amount of RNAs that formed an easily detectable clear spot. The value was calculated on the basis of the linear fitting curve, which was derived from the linear range of **ISCH-nras1** and **A647-nras1** with different amount of transfected RNAs.

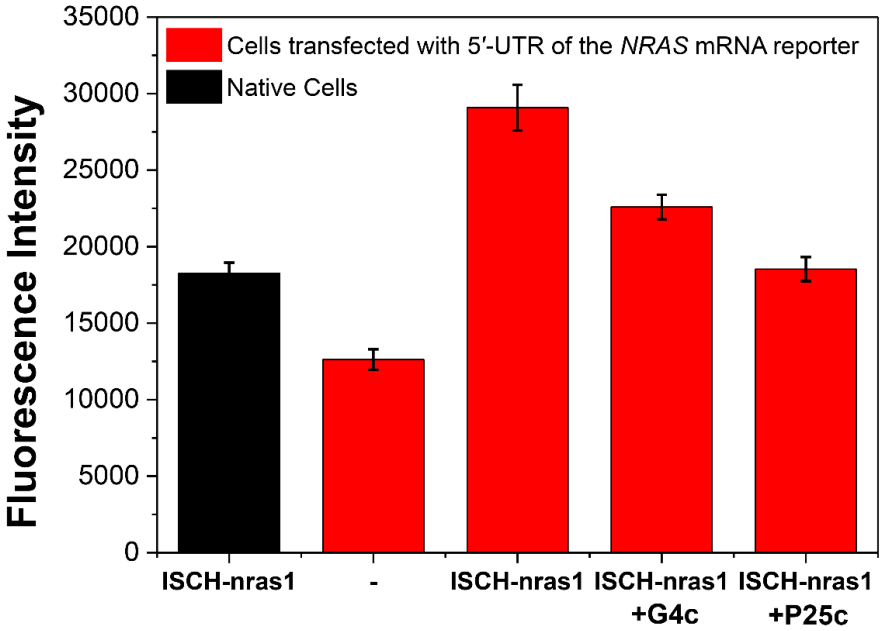

Figure S29. Quantification of the fluorescence intensity inside cells transfected with 5′-UTR of the *NRAS* mRNA reporter after treatment of **ISCH-nras1** (1 μM) with or without **G4c** (5 μM) and **P25c** (5 μM) sequences using high-content imaging platform. The data were acquired from 10000 cells per sample and three parallel experiments were performed. Emission of native cells after treatment of **ISCH-nras1** and emission of cells transfected with 5′-UTR of the *NRAS* mRNA reporter were shown as the background. As shown in the figure, enhanced fluorescence could be found in the cells transfected with the reporter after treatment of **ISCH-nras1**. Such original enhanced fluorescence signals evidently decreased by **G4c** or **P25c** treatment. **G4c** was the complementary strand to the G-rich sequence and **P25c** was the complementary strand to the tail sequence within the 5′-UTR of the *NRAS* mRNA. These findings are consistent with the results observed from the staining assays in which cells were directly transfected with RNAs.

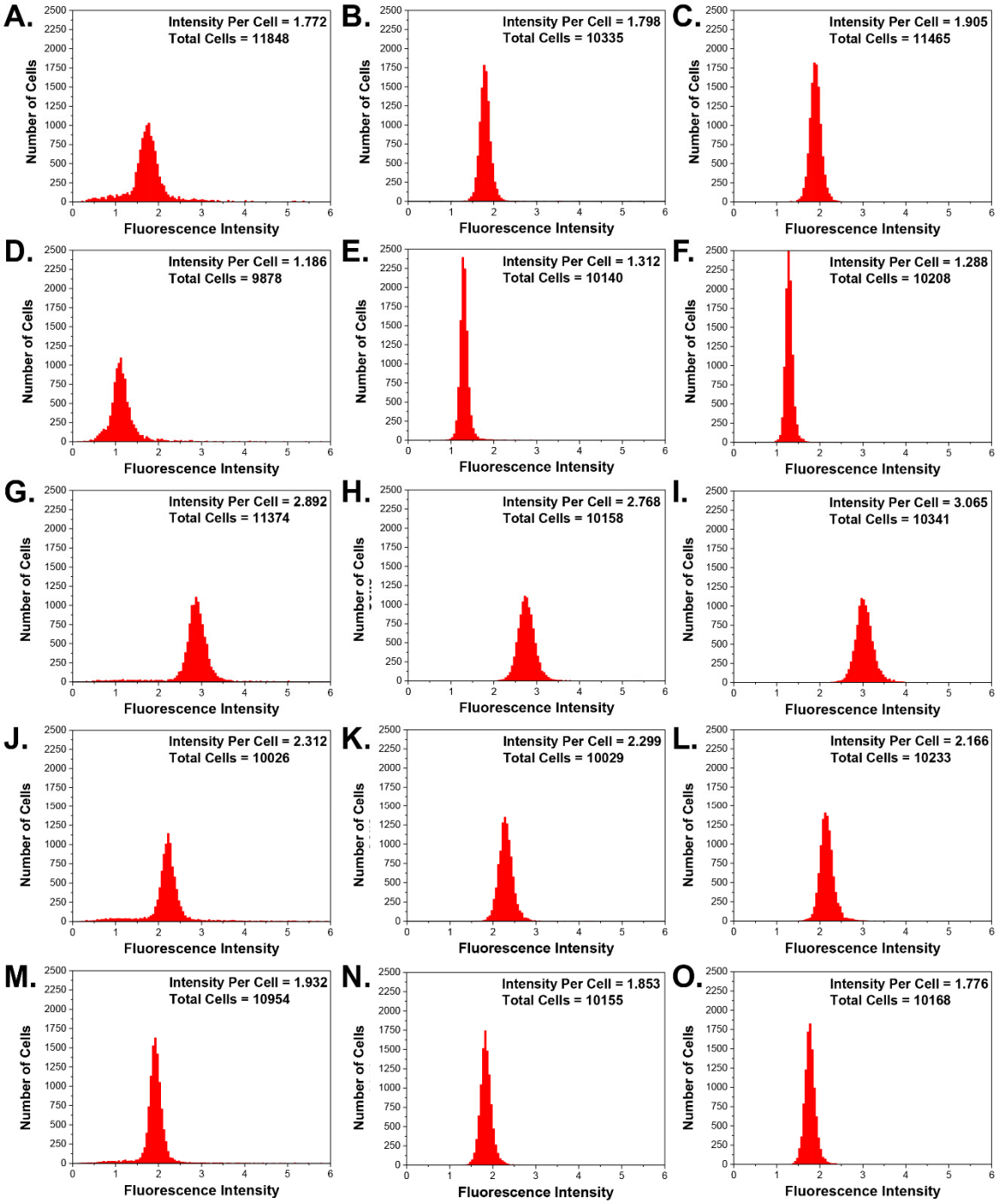

Figure S30. Histogram plotting of cell population versus corresponding fluorescence intensity quantified by high-content imaging platform. Each sample contained about 10000 cells and three parallel experiments were performed. The fluorescence intensity per cell in each sample was shown in the inner panel. (A, B, C) Histogram plotting for native cells after treatment of **ISCH-nras1**. (D, E, F) Histogram plotting for cells transfected with 5′-UTR of the *NRAS* mRNA reporter. (G, H, I) Histogram plotting for cells transfected with 5′-UTR of the *NRAS* mRNA reporter after treatment of **ISCH-nras1** (1 μM). (J, K, L) Histogram plotting for cells transfected with 5′-UTR of the *NRAS* mRNA reporter after treatment of **ISCH-nras1** (1 μM) and **G4c** (5 μM). (M, N, O) Histogram plotting for cells transfected with 5′-UTR of the *NRAS* mRNA reporter after treatment of **ISCH-nras1** (1 μM) and **P25c** (5 μM).

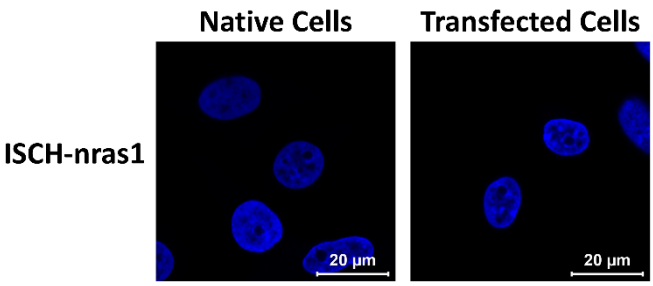

Figure S31. Confocal imaging of native cells and cells transfected with 5′-UTR of the *NRAS* mRNA reporter stained with **ISCH-nras1**.

4. References

(1) Hu, M. H.; Chen, S. B.; Guo, R. J.; Ou, T. M.; Huang, Z. S.; Tan, J. H. *Analyst* **2015**, *140*, 4616.

(2) Vorlickova, M.; Kejnovska, I.; Sagi, J.; Renciuk, D.; Bednarova, K.; Motlova, J.; Kypr, J. *Methods* **2012**, *57*, 64.

(3) Mergny, J. L.; Li, J.; Lacroix, L.; Amrane, S.; Chaires, J. B. *Nucleic Acids Res*. **2005**, *33*, e138.

(4) Dunn, K. W.; Kamocka, M. M.; McDonald, J. H. *Am. J. Physiol. Cell Physiol.* **2011**, *300*, C723.